Robust Photonic Bandgaps in Quasiperiodic and Random Extrinsic Magnetized Plasma

Chittaranjan Nayak, Carlos H. Costa, and Alireza Aghajamali

***Abstract*— In this paper, we have employed the transfer-matrix method to study theoretically the light waves propagation in extrinsic magnetized plasma multilayer, which is composed of a bulk plasma system influenced by the presence of spatially varying external magnetic field, which leads to a photonic bandgap device. The multilayered structures are arranged in periodic, quasiperiodic (Fibonacci, Octonacci, Thue–Morse, and double period), and Gaussian random fashions. The numerical results show the emergence of two main photonic bandgaps: the first gap for low frequencies and the second one for higher frequencies. We investigate the robust nature of the higher frequencies bandgap since it shows up to be invariant to different values of applied external magnetic fields and electron density as well as changes in the position and thickness of the layers introduced by the quasiperiodic and the Gaussian random sequences, respectively. The most surprising result is that this desired robust bandgap is broadening without any intermediate resonant peaks while the randomness in the layer thickness is introduced, which had not been observed in previous works about this same system.**

***Index Terms*— Electromagnetic propagation in plasma media, multilayered media, photonic bandgap materials, quasiperiodic and random media, robust bandgap.**

I. Introduction

PHOTONIC crystals (PCs) are optical materials where the dielectric permittivity is a periodic function of the space and, because of that, they are capable of controlling and manipulating the light propagation. Since the first works of Yablonovitch [1] and John [2] about PCs in 1987, several theoretical and experimental investigations have been done in order to make the photon the basic excitation of the next generation devices, i.e., by using the photon properties and its interaction with the matter for processing and transporting information [3]. The main applications of PCs are photonic optical devices such as all-optical switching and logical gates, which are essential components for computing and information processing, lasers, sensors, optical filters, Bragg's mirrors, Fabry–Perot's interferometers, among others [4], [5]. Photonic systems can also present a frequency region where the wave vector is imaginary and, consequently, the electromagnetic wave is evanescent. In this region, the wave is reflected backward and a photonic bandgap or stopband emerges. In addition, pass and defect bands can emerge as well. Then, one says that PCs have a photonic band structure that can be tuned by adjusting the geometric parameters, dielectric materials, defects, temperature, and other external effects [6].

After the initial contribution of Hojo and Mase [7], electromagnetic propagation in periodic, quasiperiodic, and random plasma photonic multilayers is a subject of great interest due to its impressive and amazing characteristics as compared to the conventional dielectric photonic multilayers. For example, the plasma PC can be designed and used as new plasma-functional devices, like frequency filters in the millimeter-wave range [8]. Recently, the light propagation on plasma photonic systems has been investigated experimentally by Fan and Dong [9], by using the dielectric barrier discharge from two liquid electrodes, and by Zhang and Ouyang [10] that used a series of gas discharge tubes. The finite-difference time-domain and the transfer-matrix methods (TMMs) were employed in order to understand, from a theoretical point of view, the new physical properties and to provide some new applications of the plasma optical materials [11]–[19]. However, the investigation of electromagnetic wave transports through an extrinsic magnetized plasma multilayer (EMPM), a bulk plasma system under the influence of periodically varying external magnetic field, is very recent and rarely explored. In general, the bulk plasma system is assumed to be a homogeneous medium, like n-GaAs, whose dielectric permittivity is influenced by an external and periodically applied magnetic field [20], [21]. Initially, King *et al.* [22] theoretically investigated the propagation of an electromagnetic wave through EMPM, which makes of this kind of system an effective photonic bandgap device in the microwave region. This remarkable result opens a new research window where an EMPM material can be used for designing of the bandgap devices that work on the microwave regime, and which can easily be extended to the terahertz frequency regime, for instance, by increasing the electron density [23]. In this context, very recent theoretical approaches such as Gaussian distributed random layer thickness [15], [16] and Octonacci [17] EMPMs have been explored with an aim to design the tunable multiband resonators.

Manuscript received July 15, 2018; revised January 5, 2019; accepted February 8, 2019. Date of publication February 26, 2019; date of current version April 10, 2019. The work of C. H. Costa was supported in part by Brazilian Research Agencies CNPq under Grant 429299/2016-8 and in part by FUNCAP under Grant BP3-0139-00177.01.00/18. The review of this paper was arranged by Senior Editor S. J. Gitomer. *(Corresponding author: Chittaranjan Nayak.)*

C. Nayak is with the Department of Electronics and Communication Engineering, SRM Institute of Science and Technology, Chennai 603202, India (e-mail: 83chittaranjan@gmail.com).

C. H. Costa is with the Universidade Federal do Ceará, Campus Avançado de Russas, Russas 62900-000, Brazil (e-mail: carloshumberto@ufc.br).

A. Aghajamali is with the Department of Physics and Astronomy, Curtin University, Perth, WA 6102, Australia (e-mail: alireza.aghajamali@gmail.com).

Color versions of one or more of the figures in this paper are available online at http://ieeexplore.ieee.org.

Digital Object Identifier 10.1109/TPS.2019.2899140

As it was mentioned, the physical properties of the constituent material have enormous effects on their band structure. The bandgap in a conventional dielectric material is a consequence of Bragg's scattering and referred to as Bragg's gap. Such bandgaps are variant to scaling and very much sensitive to disorder [24]. However, with the tremendous technological advance of manufacturing techniques in nanometric scales, artificial structures where the dispersive refractive index is negative in a given frequency region, the so-called optical metamaterials, could be experimentally fabricated and investigated [25]. It is important to mention that the metamaterials and the electromagnetic effects resulting from them had already been investigated theoretically, in 1968, by Veselago [26]. One of the most important consequences of the negative refraction index is the emergence of two new kinds of bandgaps: the "zero-$\bar{n}$" [27] and the "zero-$\bar{\phi}$" gaps [28] have been identified, where $\bar{n}$ and $\bar{\phi}$ are the average refraction index and average optical phase, respectively. The "zero-$\bar{n}$" gap appears when both the electrical permittivity $\varepsilon(\omega)$ and the magnetic permeability $\mu(\omega)$ are negative in a given frequency range, while the "zero-$\bar{\phi}$" gap emerges at the zero effective phase delay point [29]. In dispersive materials with ε-negative and μ-positive [30] or vice-versa [31], the bandgaps are found not being scale length invariant. In contrast to the conventional and well-investigated Bragg's gap, both the "zero-$\bar{n}$" and the "zero-$\bar{\phi}$" gaps remain invariant to the change in scale length and they are also robust against disorder [32]. Besides that, two more types of such robust photonic bandgaps, namely, the "zero-μ" and the "zero-ε" gaps, were recently studied. However, these bandgaps appear only for oblique incidence and for a particular light wave polarization: the first one occurs only for s-polarized waves, whereas the latter occurs only for p-polarized waves [33]. Recent investigations on non-Bragg's bandgaps, such as, effect of incident angle over the "zero-$\bar{n}$" gap [34], and the effect of loss factor over the "zero-μ" gap and the "zero-ε" gap [35] of the double negative metamaterial multilayer, provide a new way to study the invariable and the robust nature of these gaps.

In this paper, we investigate how the robustness of the bandgaps on EMPMs change with the position of the layers, the spatial arrangement of these layers, the external magnetic field intensity, and the electron density. Moreover, the very useful wider bandgap is also investigated while introducing some randomness in the layer thickness. To do so, we numerically calculate the light transmittance by using the well-established and powerful TMM method [36] in some basic 1-D PCs such as periodic, Fibonacci (FB), Thue–Morse (TM), double period (DP) [37], Octonacci [17], [38], and Gaussian distributed random layer thickness [15], [16], [39] multilayers.

This paper is organized as follows. In Section II, we discuss the theoretical model with emphasis on the description of the EMPM systems. Also, we present the quasiperiodic sequences and random multilayers considered, and the TMM method, which is used to simplify the algebra that can be hard to deal with otherwise. Our results about the transmittance spectra of light as well a detailed discussion over them are in Section III. Basically, we are concerned into investigate the effects of the layer position and of the randomness in layer thickness (in Section III-A), as well as, the external magnetic field intensity (in Section III-B), and the electron density (in Section III-C) on the higher frequency bandgap. Finally, our findings are summarized in Section IV.

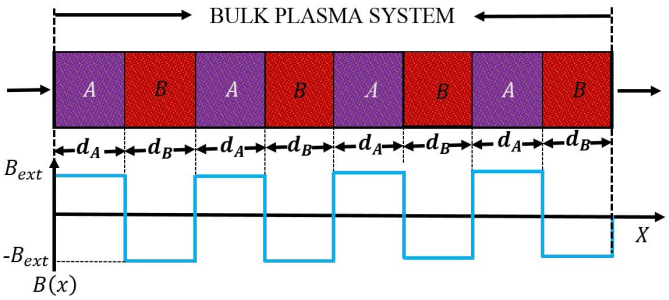

Fig. 1. (Color online) Schematic showing the geometry of a periodic EMPM system considered in this paper having $N = 4$.

II. General Theory

The geometric scheme of a 1-D periodic EMPM is presented in Fig. 1. The magnetized plasma material is characterized by an electrical permittivity that depends on both frequency ω and magnetic field intensity $B(x)$, which varies with the position x, and it is given in [40]

$$\varepsilon_{\mathrm{MP}}(\omega, B(x)) = 1 - \left[\frac{\omega_p^2}{\omega^2\left(1 - i\frac{\gamma}{\omega} \mp \frac{\omega_l}{\omega}\right)}\right] \tag{1}$$

where $\omega_p = (n_e e^2/m_e\varepsilon_0)^{1/2}$, $\omega_l = eB(x)/m_e$, and γ are the plasma, the gyro-magnetic, and the effective collision frequencies, respectively. Also, e, n_e, and m_e are the electron charge, density, and mass, respectively, while ε_0 is the permittivity of the free space. In addition, the magnetic permeability of the magnetized plasma considered in this paper is assumed, for simplicity, to be nondispersive and is given by $\mu_{\mathrm{MP}} = 1$.

As it is shown in Fig. 1, the regions of space in which the magnitude of the magnetic field is assumed to be constant and positive, i.e., $B(x) = +B_{\mathrm{ext}}$, define medium A, with thickness d_A and dielectric permittivity ε_A and a such medium is considered right-hand polarization (RHP). However, for regions of space where the magnitude of the magnetic field is considered to be also constant but negative, i.e., $B(x) = -B_{\mathrm{ext}}$, we have the medium B, whose thickness and dielectric permittivity are d_B and ε_B, respectively, and so it is considered left-hand polarization (LHP) [22]. Such periodic variation of permittivity of the considered bulk plasma system can be treated as a periodic EMPM, namely, air$|(A|B)^N|$air, where N means the number of times that the unit cell $A|B$, for a periodic case, is repeated: we have $N = 4$ in Fig. 1. The size of the PC is given by $D = Nd$, where d is the thickness of the unit cell ($d = d_A + d_B$ in Fig. 1).

In addition, an aperiodic multilayer can be classified in two types: the deterministic, or the quasiperiodic, and the random multilayers. Some of the well-known quasiperiodic structures that were considered in this investigation are FB, TM, DP, and Octonacci and their respective inflation rules are: $A \to AB$, $B \to A$ (for FB); $A \to AB$, $B \to BA$ (for TM); $A \to AB$, $B \to AA$ (for DP), and $A \to B$, $B \to BAB$ (for Octonacci) [37], [38]. The other category of

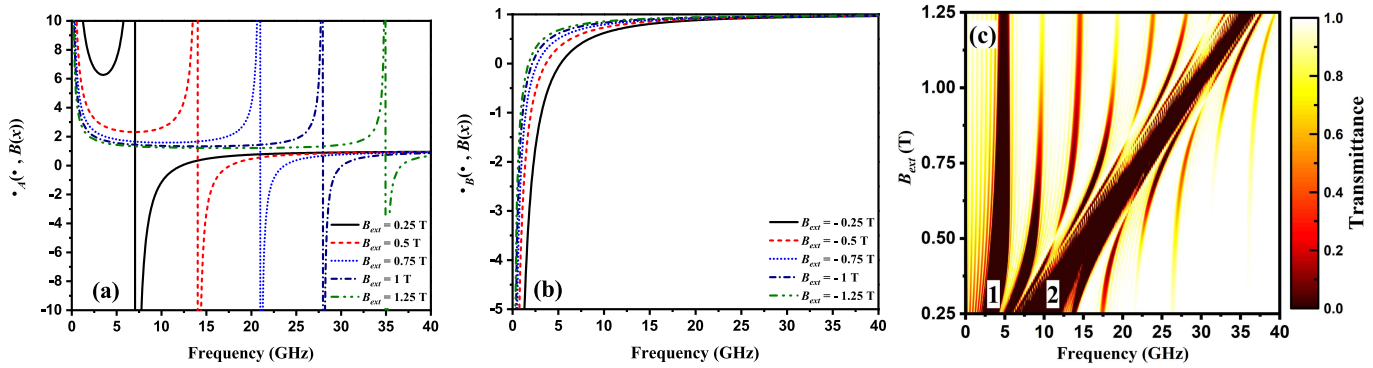

Fig. 2. (Color online) Permittivity of the magnetized plasma material versus the frequency for different values of external magnetic fields considering (a) RHP and (b) LHP configurations. (c) Plot of transmittance versus the frequency and the external magnetic field for periodic ($N = 8$) EMPMs.

aperiodic multilayers is purely random. The randomness in the multilayer can be introduced by using different mathematical and statistical approaches. The random multilayers were very recently investigated by using different random sequences, random distributions (i.e., uniform or Gaussian) [15], [16], and permutation rules [41] (i.e., the probability of occurrences of the layer). Here, the Gaussian distributed random multilayer is taken into account. Such a random structure is a disordered 1-D photonic system in which the disorder is obtained with a random variation of the thickness of the layers in a periodic structure. Moreover, the probability of the random thicknesses of the layers to occur follows a Gaussian function, centered at some mean value and with a standard deviation σ. By using the mathematical formulation for these quasiperiodic sequences and Gaussian distributed random multilayers, the position and the width of the layer are adjusted and designed accordingly in order to obtain the desired effects in EMPM.

A. Mathematical Formulation

Among many theoretical approaches that are employed to calculate the light propagation spectra through any of the multilayered systems presented previously, the TMM is widely adopted due to its simplicity, it does not require an expensive computational resource and because its numerical results are in very good agreement with the experimental ones [42], [43]. According to Born and Wolf [36], the 2×2 transfer matrix M of a multilayered system is given by

$$M = \begin{bmatrix} M_{11} & M_{12} \\ M_{21} & M_{22} \end{bmatrix} = D_0^{-1} \left[\prod_{j=1}^{M} D_j P_j D_j^{-1} \right] D_0 \qquad (2)$$

where M_{11}, M_{12}, M_{21}, and M_{22} are the transfer-matrix elements. P_j and D_j denote the propagation matrix and dynamic matrix of the jth slab having thickness d_j and permittivity ε_j, respectively. D_0 in (2) is the dynamic matrix for the surrounded medium, that is considered as air in this paper. For normal incidence, the general mathematical equation for P_j and D_j are given as [22] (c is the light speed in vacuum)

$$P_j = \begin{bmatrix} \exp(i\omega\sqrt{\varepsilon_j} d_j/c) & 0 \\ 0 & \exp(-i\omega\sqrt{\varepsilon_j} d_j/c) \end{bmatrix} \qquad (3)$$

$$D_j = \begin{bmatrix} 1 & 1 \\ \sqrt{\varepsilon_j} & \sqrt{\varepsilon_j} \end{bmatrix}. \qquad (4)$$

We now intend to numerically obtain the transfer matrices M for periodic, quasiperiodic, and Gaussian distributed random layer thickness EMPMs. From (2), it is observed that the transfer matrix M of any multilayer is formed by the product of the transfer matrices of each individual layers. Moreover, the order of the matrices depends on the sequence under consideration. Therefore, by following the periodic, quasiperiodic, and random arrangements, it is quite easy to present the mathematical modeling of such EMPM. The transmittance T for a given multilayered system is $T = |1/M_{11}|^2$ [38].

III. Numerical Results and Discussion

In this section, we present the numerical results regarding the propagation of electromagnetic waves on EMPMs. We consider only normally incident waves to the interfaces. The physical parameters for magnetized plasma are taken from [15]–[18], i.e., $n_e = 8 \times 10^{17}$ m^{-3}, which gives $\omega_p \approx 50.45 \times 10^9$ rad/s. The effect of the collision frequency γ is not included in these numerical simulations because of its negligible impact on the transmittance spectra [15]–[17]. The individual layers have thicknesses equal to 15 mm. We consider $N = 8$ for the periodic structure, which gives a structure with 16 slabs.

In Fig. 2(a), we plot the dispersive dielectric funcion ε_A versus the frequency for an LHP, considering different values of B_{ext}. One can observe that, for $\omega < \omega_l$, we have $\varepsilon_A > 0$ and the plasma layer behaves as a dielectric material. Otherwise, if $\omega > \omega_l$, we have $\varepsilon_A < 0$ and the plasma media is a negative-ε material. Also, we note that ε_A decreases as the magnitude of B_{ext} increases. The dispersive dielectric function for an RHP, ε_B, is presented in Fig. 2(b), and we observe that for $\omega < [-\omega_l + (\omega_l^2 + 4\omega_p^2)^{1/2}]/2$, the plasma layer behaves as a ε-negative material. Otherwise, it has a dielectric behavior as well.

The transmission spectra of a periodic EMPM were calculated and it is shown in Fig. 2(c) as a function of the frequency and the external magnetic field. Two broad bandgaps, labeled as 1 and 2, are observed within the considered frequency range and the magnetic field has a strong effect on them, once these bandgaps are blue shifted and becomes narrower as B_{ext} increases. In Fig. 2(a) and (b), we can observe a higher refractive index contrast mainly for frequencies around 3 GHz, for $B_{\text{ext}} = 0.25$ T, and the bandgap named as

TABLE I

BANDWIDTHS OF THE GAPS 1 AND 2 IN PERIODIC ($N = 8$) EMPM FOR DIFFERENT VALUES OF B_{EXT} [SEE FIG. 2(C)]

B_{ext}	Bandgap 1	Bandgap 2
0.25 T	2.17 – 4.13 GHz	6.77 – 12.16 GHz
0.5 T	3.29 – 5.37 GHz	13.88 – 17.99 GHz
0.75 T	3.84 – 5.49 GHz	20.99 – 23.31 GHz
1 T	4.13 – 5.45 GHz	27.97 – 30.15 GHz
1.25 T	4.33 – 5.37 GHz	35.09 – 36.80 GHz

1 emerges. However, the bandgap named as 2, which appears around 10 GHz, is a zero-$\bar{n}$ gap, and we expect that this gap presents some robust behavior [see Fig. 2(c)]. The observed functionality of bandgap over the magnetic field B_{ext} is very general and obvious [15], [45]. The notable impact of this observation is the difference between the slope of blue shifts of the bandgaps labeled as 1 and 2, as shown in Fig. 2(c). The bandwidth and the position of these two bandgaps for some values of B_{ext} are given in Table I. The observed change in slope of blue shift may partially dependent on the geometrical parameter of the considered structure, but instead, this happens because of the frequency- and magnetic field-dependent dielectric permittivity of the magnetized plasma material. In addition, as B_{ext} increases, new narrow bandgaps emerges and they have the same origin as the conventional Bragg's gaps.

Regarding the effect of scale length changes over the emerged bandgaps, it is known that they depend on the layer width [45]. However, a recent investigation about this topic, Nayak *et al.* [15] reported that with the introduction of randomness in the layer thickness deface the first bandgap (below plasma frequency bandgap) of the full plasma multilayer system, shown in Fig. 2(c). Specifically, deface of the bandgap appears in the form of a wider bandgap with few resonant peaks. It is important to mention that the computational analysis of the higher frequency range bandgap (above plasma frequency bandgap) is out of its scope of this paper and this is the object of another investigation. Furthermore, the nature of the dispersion relation of the constituent material has an ability to origin some novel and more interesting results. Therefore, in the next sections, the effects of the layer position and of the randomness in layer thickness (in Section III-A), as well as, the external magnetic field intensity (in Section III-B), and the electron density (in Section III-C) on the higher frequency bandgap are presented and discussed. This higher frequency bandgap has a lower band edge at 27.97 GHz and higher band edge at 30.15 GHz for $B_{\text{ext}} = 1$ T (see Table I).

A. Effects of Quasiperiodic and Random Layer Thickness Multilayers

In this section, we consider $B_{\text{ext}} = 1$ T and the frequency range is fixed to 27.5–32.5 GHz, which corresponds to the higher bandgap region. For the quasiperiodic sequences, we consider the following unit cells: $A|B|A|A|B|A|B|A|A|B|A|A|B$, that corresponds to the sixth generation of FB sequence; $A|B|B|A|B|A|A|B|B|A|A|B|A|B|B|A$, that corresponds to the fourth generation of TM sequence;

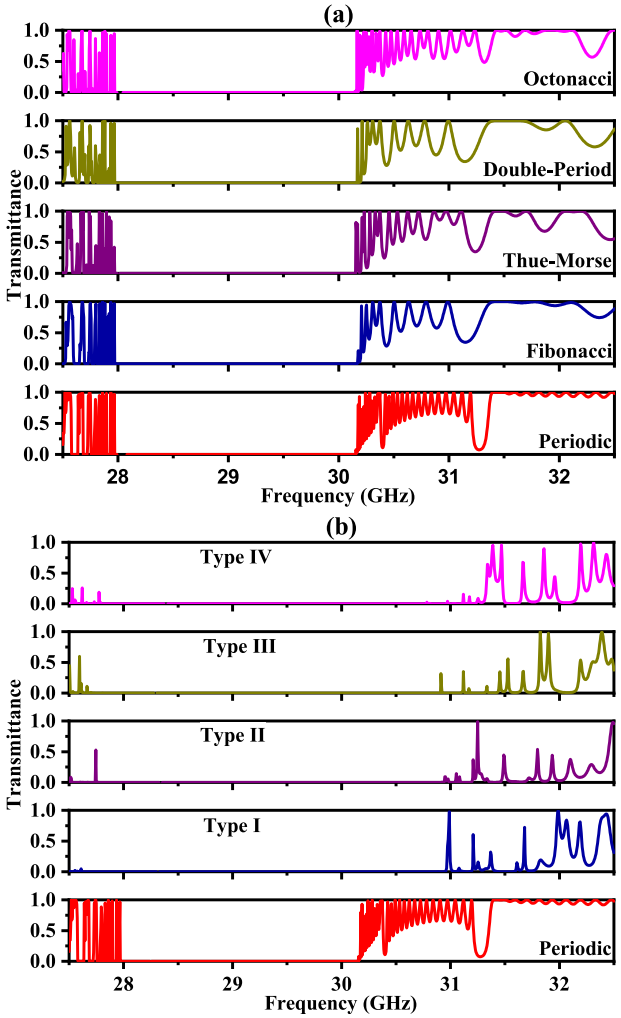

Fig. 3. (Color online) (a) Transmission spectra of periodic ($N = 8$), FB, TM, DP, and Octonacci EMPMs with $B_{\text{ext}} = 1$ T. (b) Same as (a), but for a set of four possible Gaussian distributed random layer thickness 32 layer EMPMs along with the periodic structure.

$A|B|A|A|A|B|A|B|A|B|A|A|A|B|A|A$, that is the fourth generation of DP sequence; and, finally, we consider the fifth generation of Octonacci sequence, whose multilayer is given by $B|A|B|B|A|B|B|A|B|B|A|B|B|B|A|B$. The generation numbers were chosen in order to obtain a multilayer whose unit cell has exactly 16 slabs. The only exception is the FB sequence that has just 13 slabs. From these considered sequences, it was well examined that the position and the count of two types of layer (A and B) are inconsistent due to their deterministic mathematical formulation rules.

The transmission spectra of all the quasiperiodic sequences along with the periodic ($N = 8$) structure are presented in Fig. 3(a). It is interesting to note that the wider bandgap for all the quasiperiodic sequences is alike to the bandgap that appears in case of the periodic structure. Therefore, we can conclude that this bandgap is independent of sequence considered, unlike what occurs with the bandgaps in conventional periodic dielectric multilayers. This is a consequence of the dependence of the dielectric permittivity of magnetized plasma multilayers on the frequency and the magnetic field [46].

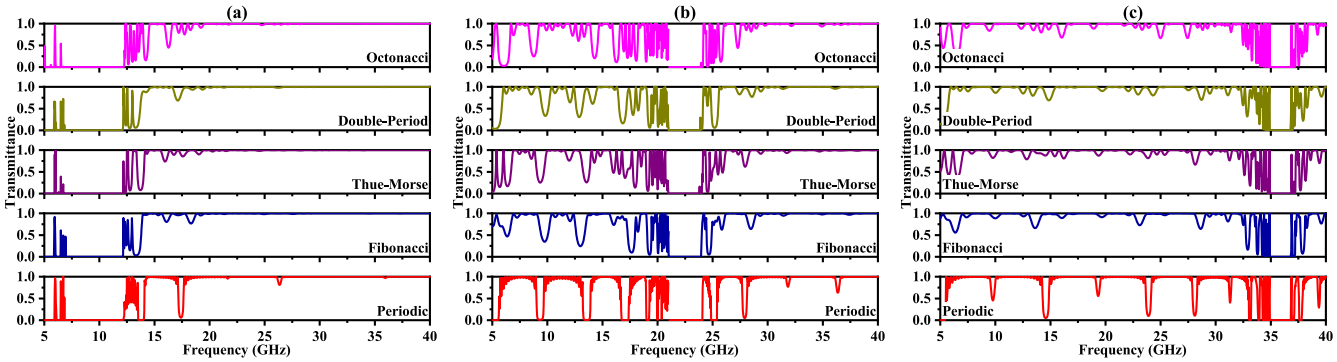

Fig. 4. (Color online) Transmission spectra of periodic ($N = 8$), FB, TM, DP, and Octonacci EMPMs having (a) $B_{\text{ext}} = 0.25$ T, (b) $B_{\text{ext}} = 0.75$ T, and (c) $B_{\text{ext}} = 1.25$ T.

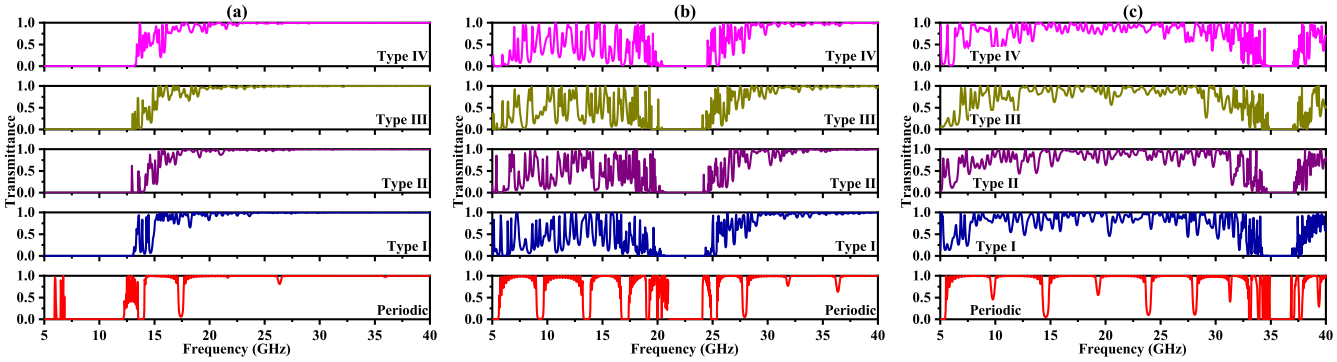

Fig. 5. (Color online) Transmission spectra of a set of four possible Gaussian distributed random layer thickness 32 layer EMPMs along with the periodic structure ($N = 16$) having (a) $B_{\text{ext}} = 0.25$ T, (b) $B_{\text{ext}} = 0.75$ T, and (c) $B_{\text{ext}} = 1.25$ T.

Similarly, the occurrence of a robust bandgap against the randomness in the layer thickness is also investigated. To do so, a set of four possible 32 layered Gaussian distributed random layer thickness EMPMs (named Types I–IV) are considered and, because of this, the periodic unit cell is repeated 16 times, i.e., $N = 16$ when we deal with random structures. The considered mean value of the layer thickness is 15 mm, while the considered standard deviation σ of the distribution is assumed to be 6 mm. The transmittance spectra of four possible 32 layered Gaussian distributed random layer thickness EMPMs along with the periodic ($N = 16$) structure are depicted in Fig. 3(b). It is observed that the zero transmittance region that is the higher frequency bandgap for the random EMPM is wider than the bandgap provided by the periodic EMPM (which corresponds to $\sigma = 0$). Moreover, some resonant peaks appear outside the boundary of the bandgap provided by the periodic structure. Therefore, we can observe that the aroused bandgap of the periodic structure enlarges while encountering by the random variation in layer thickness.

These effects on the bandgap, while the introduction of randomness in the layer thickness, are similar to the results presented by Nayak *et al.* [15]. Unlike as it was reported, no intermediate resonant peaks or the so-called defect modes have appeared within the considered bandgap. The appearance of such extraordinary change from the previous results is due to the under considered frequency range which transfigures the optical length between the individual layers of the multilayer. This may subjugate the appearances of the defect modes, which are assumed to be aroused while the introduction of randomness in layer thickness [15], [39]. Therefore, one can conclude that the introduction of randomness in the layer thickness can be employed to enlarge the specific higher frequency bandgap of the proposed EMPM. The bandwidths of the wider bandgap in quasiperiodic and random EMPMs for $B_{\text{ext}} = 1$ T are given in Table II, and we observe a robust bandgap from 27.99 to 30.15 GHz regardless how the slabs A and B are spatially arranged or if their thicknesses have a small variation around a average thickness.

TABLE II

BANDWIDTHS, IN GIGAHERTZ, IN QUASIPERIODIC AND RANDOM EMPMS FOR $B_{\text{EXT}} = 1$ T (SEE FIG. 3)

Quasiperiodic		Random	
Structure	Bandwidth	Structure	Bandwidth
Periodic ($N = 8$)	27.97 - 30.15	Periodic ($N = 16$)	27.97 - 30.16
Fibonacci	27.99 - 30.17	Type I	27.70 - 33.33
Thue-Morse	27.98 - 30.15	Type II	27.75 - 30.43
Double-period	27.97 - 30.17	Type III	27.78 - 30.41
Octonacci	27.97 - 30.15	Type IV	27.79 - 30.78

B. Effect of the Magnetic Field Intensity

In the following, we demonstrate explicitly the validity of the results above presented for some values of magnetic field B_{ext}. To do so, the same set of quasiperiodic sequences [as in Fig. 3(a)] and Gaussian distributed random structures [as in Fig. 3(b)] are considered. The transmittance spectra for periodic structure ($N = 8$) and quasiperiodic sequences are shown in Fig. 4. Fig. 4(a)–(c) corresponds to $B_{\text{ext}} = 0.25$ T, $B_{\text{ext}} = 0.75$ T, and $B_{\text{ext}} = 1.25$ T, respectively. By analyzing the transmittance spectra of the periodic structure, one can note that the aroused bandgap is a function of external magnetic

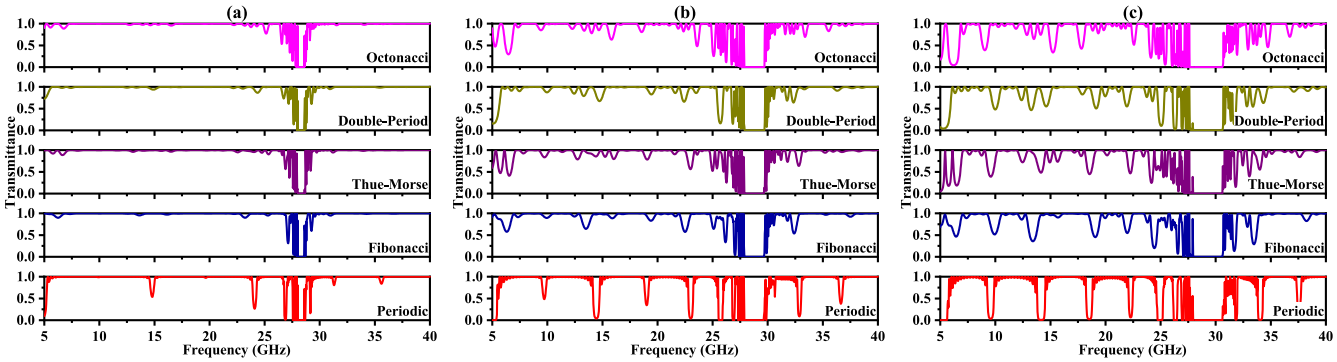

Fig. 6. (Color online) Transmission spectra of periodic ($N = 8$), FB, TM, DP, and Octonacci EMPMs having (a) $n_e = 2\times10^{17}$ m^{-3}, (b) $n_e = 6\times10^{17}$ m^{-3}, and (c) $n_e = 10\times10^{17}$ m^{-3}.

field intensity B_{ext} as it was said before [see the comments about Fig. 2(c)]. Similar transmittance spectra are observed for all the considered quasiperiodic sequences. In addition, for a specific magnetic field intensity B_{ext}, the bandgaps have the same width and they are localized at the same frequency region. Excluding the general dependence of B_{ext}, these topological features of the aroused bandgaps confirm that they are invariant under any changes in layer position and the count of the types of layers.

The effects of magnetic field on the bandgap aroused by a set of Gaussian distributed random layer thickness 32 layer structures were investigated and the results are shown in Fig. 5. The transmittance spectra of the considered structure along the periodic multilayer ($N = 16$) for the different values of magnetic field B_{ext} are shown in Fig. 5(a)–(c), for $B_{\text{ext}} = 0.25$ T, $B_{\text{ext}} = 0.75$ T, and $B_{\text{ext}} = 1.25$ T, respectively. From these figures, a general magnetic field intensity bandgap tunability is observed the same as in the case of quasiperiodic structures [15]–[17]. Moreover, as demonstrated at $B_{\text{ext}} = 1$ T [Fig. 3(b)], a similar behavior of the transmittance is noted for the magnetic field B_{ext} values, i.e., the aroused bandgap becomes wider as compared to the periodic structure. Therefore, from all the results presented until here, we conclude that the Gaussian distributed random layer thickness plasma multilayers are able to provide wider bandgap as compared to the bandgap provided by the conventional periodic plasma multilayers. Table III presents the bandwidths, in gigahertz, of the wider gap in quasiperiodic (on top) and random (on bottom) EMPMs for different values of B_{ext} according to Figs. 4 and 5. For $B_{\text{ext}} = 0.25$, 0.75, and 1.25 T, we found the respective frequency ranges that correspond a robust bandgap for periodic, quasiperiodic, and random EMPMs, for each of the values of B_{ext} considered: 9.24–12.08 GHz, 21.15–23.85 GHz, and 34.99–36.78 GHz.

TABLE III

BANDWIDTHS, IN GIGAHERTZ, IN QUASIPERIODIC AND RANDOM EMPMS FOR DIFFERENT VALUES OF B_{EXT}, IN T. (SEE FIGS. 4 AND 5)

Quasiperiodic			
Structure	$B_{ext} = 0.25$	$B_{ext} = 0.75$	$B_{ext} = 1.25$
Periodic ($N = 8$)	6.97 - 12.15	21.15 - 23.88	34.99 - 36.78
Fibonacci	6.92 - 12.11	21.01 - 23.88	34.97 - 36.81
Thue-Morse	6.92 - 12.08	21.08 - 23.85	34.94 - 36.82
Double-period	6.93 - 12.11	21.01 - 23.85	34.99 - 36.78
Octonacci	6.86 - 12.18	21.05 - 23.92	34.93 - 36.84
Random			
Structure	$B_{ext} = 0.25$	$B_{ext} = 0.75$	$B_{ext} = 1.25$
Periodic ($N = 16$)	9.24 - 12.20	20.98 - 24.06	34.99 - 36.81
Type I	1.49 - 12.76	20.49 - 24.20	34.60 - 37.20
Type II	1.57 - 12.64	20.38 - 24.02	34.37 - 37.13
Type III	1.09 - 13.02	20.08 - 24.13	34.78 - 36.99
Type IV	1.61 - 12.68	20.70 - 23.99	34.64 - 36.99

C. Effect of the Electron Density

Finally, but not less important, we investigate numerically the effect of electron density n_e on the higher frequency bandgap. Here, we consider $B_{\text{ext}} = 1$ T, and the same EMPMs, namely, periodic, quasiperiodic, and Gaussian distributed random layer thickness structures. In Fig. 6, we have the effect of electron density for the periodic ($N = 8$) and quasiperiodic structures for: 1) $n_e = 2\times10^{17}$ m^{-3}; 2) $n_e = 6\times10^{17}$ m^{-3}; and 3) $n_e = 10\times10^{17}$ m^{-3}. We note that the transmittance spectra of the periodic structures, besides a blue shift of the right edge bandgap, we have also that width of the bandgap corresponding becomes wider as the electron density n_e increases. These effects are similar to those ones mentioned by Dehnavi *et al.* [45] and, likely the effects of magnetic field intensity on higher bandgap, they occur due to the changes in the dielectric permittivity dielectric constant of the magnetized plasma material. At the same time, as depicted in Fig. 3(a), the bandgaps formed by the periodic multilayer remain invariant against the change of the layer position and the number of layers of each quasiperiodic sequence, for all the values of electron density considered here.

In Fig. 7, we present the same as shown in Fig. 6, but for the Gaussian distributed random layer thickness 32-layer structure along with the periodic ($N = 16$) one. Like as in Fig. 5, a similar effect caused by the electron density n_e is observed: for all the random multilayers considered, wider bandgaps compared to those ones provided by the periodic multilayer, are obtained. These results on the dependence of the transmittance spectrum on the electron density confirm that the presence of randomness in the layer thickness of magnetized plasma multilayer is capable to enlarge the aroused bandgap. Table IV presents the bandwidths, in gigahertz, of the wider gap in quasiperiodic (on top) and random (on bottom) EMPMs for different values of n_e according to Figs. 6 and 7. For $n_e = 2\times10^{17}$, 6×10^{17}, and 10×10^{17} m^{-3}, we found the

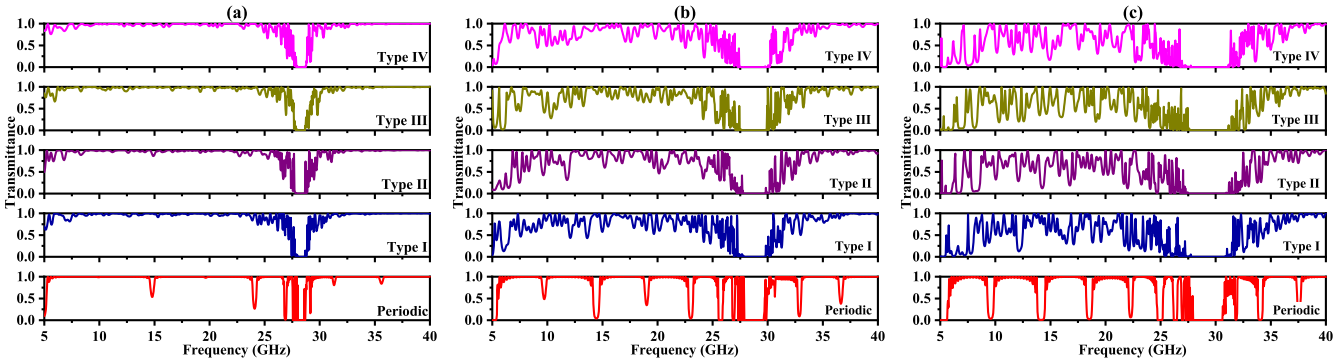

Fig. 7. (Color online) Transmission spectra of a set of four possible Gaussian distributed random layer thickness 32 layer EMPMs along with the periodic structure ($N = 16$) having (a) $n_e = 2 \times 10^{17}$ m^{-3}, (b) $n_e = 6 \times 10^{17}$ m^{-3}, and (c) $n_e = 10 \times 10^{17}$ m^{-3}.

TABLE IV

BANDWIDTHS, IN GIGAHERTZ, IN QUASIPERIODIC AND RANDOM EMPMS FOR DIFFERENT VALUES OF n_e, IN $\times 10^{17}$ m^{-3} (SEE FIGS. 6 AND 7)

Quasiperiodic			
Structure	$n_e = 2$	$n_e = 6$	$n_e = 10$
Periodic ($N = 8$)	28.02 - 28.51	27.95 - 29.63	28.09 - 30.61
Fibonacci	28.02 - 28.58	27.98 - 29.66	27.95 - 30.61
Thue-Morse	28.02 - 28.51	27.95 - 29.63	27.95 - 30.61
Double-period	28.09 - 28.58	27.98 - 29.66	28.02 - 30.58
Octonacci	28.09 - 28.58	27.98 - 29.66	27.84 - 30.61
Random			
Structure	$n_e = 2$	$n_e = 6$	$n_e = 10$
Periodic ($N = 16$)	28.12 - 28.58	27.98 - 29.63	27.98 - 30.61
Type I	27.98 - 28.65	27.06 - 29.80	27.77 - 30.89
Type II	27.88 - 28.65	27.90 - 29.91	27.60 - 30.93
Type III	27.95 - 28.65	27.74 - 29.81	27.63 - 31.10
Type IV	27.98 - 28.65	27.67 - 29.70	27.74 - 31.14

respective frequency ranges that correspond a robust bandgap for periodic, quasiperiodic, and random EMPMs, for each of the values of n_e considered: 28.09–28.51 GHz, 27.98–29.63 GHz, and 28.09–30.58 GHz.

IV. CONCLUSION

In summary, we have investigated the light transmittance in extrinsic plasma photonic multilayer and present some results that show the emergence of a robust bandgap. This bandgap is invariant against the different types of multilayered structures, such as periodic, quasiperiodic (FB, TM, DP, and Octonacci), and random (Gaussian distributed random layer thickness) magnetized plasma multilayer for a range of magnetic field B_{ext} and also electron density n_e. The numerical results show that a wider bandgap emerges while we incorporate some randomness in the layer thickness of an EMPM. Moreover, we found that the magnetic field B_{ext} as well as the electron density n_e can be properly adjusted in order to tune the photonic bandgaps in disordered multilayers. For quasiperiodic structures, is was shown that the higher bandgap is invariant or robust for fixed values of B_{ext} and n_e, while it becomes wider for Gaussian distributed random layer thickness multilayers. As the most surprising result of our investigation we found that, for the same photonic structure, one can have, or not, a multichannel structure with several resonant transmission peaks if we use quasiperiodic or random structures just adjusting one or more of these external effects and parameters, i.e., that resonant peaks can be switched on or off in very simple ways. This behavior is very useful and desired for applications of multiplex logic gates.

We hope these very interesting results can encourage and inspire experimental groups to fabricate and experimentally investigate such robust bandgaps in 1-Dextrinsic magnetized plasma PCs.

ACKNOWLEDGMENT

The author C. Nayak would like to thank the Vice Chancellor, SRM Institute of Science and Technology, Chennai, for his continuous encouragement in this paper. The authors would like to thank Dr. S. Routray, SRM Institute of Science and Technology, Chennai, and Dr. F. Scotognella, Politecnico di Milano, Milan, for useful suggestions and discussions.

REFERENCES

[1] E. Yablonovitch, "Inhibited spontaneous emission in solid-state physics and electronics," *Phys. Rev. Lett.*, vol. 58, no. 20, pp. 2059–2062, May 1987.
[2] S. John, "Strong localization of photons in certain disordered dielectric superlattices," *Phys. Rev. Lett.*, vol. 58, no. 23, pp. 2486–2489, Jun. 1987.
[3] D. Thomson *et al.*, "Roadmap on silicon photonics," *J. Opt.*, vol. 18, no. 7, Jun. 2016, Art. no. 073003.
[4] Q. Gong and X. Hu, Eds., *Photonic Crystals: Principles and Applications*, 1st ed. Boca Raton, FL, USA: CRC Press, 2014.
[5] A. Vakhrushev, Ed., *Theoretical Foundations and Application of Photonic Crystals*, 1st ed. London, U.K.: IntechOpen, 2018.
[6] C. Soukoulis, Ed., *Photonic Band Gap Materials*, 1st ed. London, U.K.: Kluwer, 1996.
[7] H. Hojo and A. Mase, "Dispersion relation of electromagnetic waves in one-dimensional plasma photonic crystals," *J. Plasma Fusion Res.*, vol. 80, no. 2, pp. 89–90, Jul. 2004.
[8] B. Suthar and A. Bhargava, "Optical properties of plasma photonic crystals," *Silicon*, vol. 7, no. 4, pp. 433–435, Mar. 2015.
[9] W. Fan and L. Dong, "Tunable one-dimensional plasma photonic crystals in dielectric barrier discharge," *Phys. Plasmas*, vol. 17, no. 7, Jul. 2010, Art. no. 073506.
[10] L. Zhang and J.-T. Ouyang, "Experiment and simulation on one-dimensional plasma photonic crystals," *Phys. Plasmas*, vol. 21, no. 10, Oct. 2014, Art. no. 103514.
[11] C.-Z. Li, S.-B. Liu, X.-K. Kong, H.-F. Zhang, B.-R. Bian, and X.-Y. Zhang, "A novel comb-like plasma photonic crystal filter in the presence of evanescent wave," *IEEE Trans. Plasma Sci.*, vol. 39, no. 10, pp. 1969–1973, Oct. 2011.
[12] L. Qi, Z. Yang, and T. Fu, "Defect modes in one-dimensional magnetized plasma photonic crystals with a dielectric defect layer," *Phys. Plasmas*, vol. 19, no. 1, Jan. 2012, Art. no. 012509.
[13] H.-F. Zhang, S.-B. Liu, and X.-K. Kong, "Photonic band gaps in one-dimensional magnetized plasma photonic crystals with arbitrary magnetic declination," *Phys. Plasmas*, vol. 19, no. 12, p. 122103, Dec. 2012.

[14] Z. H. Feng, S.-B. Liu, and X.-K. Kong, "Enlarged omnidirectional band gap in one-dimensional plasma photonic crystals with ternary Thue–Morse aperiodic structure," *Phys. B, Condens. Matter*, vol. 410, pp. 244–250, Feb. 2013.
[15] C. Nayak, A. Aghajamali, F. Scotognella, and A. Saha, "Effect of standard deviation, strength of magnetic field and electron density on the photonic band gap of an extrinsic disorder plasma photonic structure," *Opt. Mater.*, vol. 72, pp. 25–30, Oct. 2017.
[16] C. Nayak, A. Aghajamali, and A. Saha, "Double-negative multilayer containing an extrinsic random layer thickness magnetized cold plasma photonic quantum-well defect," *Superlattices Microstruct.*, vol. 111, pp. 248–254, Nov. 2017.
[17] C. Nayak, A. Aghajamali, T. Alamfard, and A. Saha, "Tunable photonic band gaps in an extrinsic octonacci magnetized cold plasma quasicrystal," *Phys. B, Condens. Matter*, vol. 525, pp. 41–45, Nov. 2017.
[18] H. Tan, C. Jin, L. Zhuge, and X. Wu, "Simulation on the photonic bandgap of 1-D plasma photonic crystals," *IEEE Trans. Plasma Sci.*, vol. 46, no. 3, pp. 539–544, Mar. 2018.
[19] C. Nayak, A. Saha, and A. Aghajamali, "Periodic multilayer magnetized cold plasma containing a doped semiconductor," *Indian J. Phys.*, vol. 92, no. 7, pp. 911–917, Jul. 2018.
[20] C. Xu, D. Han, X. Wang, X. Liu, and J. Zi, "Extrinsic photonic crystals: Photonic band structure calculations of a doped semiconductor under a magnetic field," *Appl. Phys. Lett.*, vol. 90, no. 6, Feb. 2007, Art. no. 061112.
[21] T.-C. King, C.-C. Wang, W.-K. Kuo, and C.-J. Wu, "Analysis of effective plasma frequency in a magnetized extrinsic photonic crystal," *IEEE Photon. J.*, vol. 5, no. 6, Dec. 2013, Art. no. 2700706.
[22] T.-C. King, C.-C. Yang, P.-H. Hsieh, T.-W. Chang, and C.-J. Wu, "Analysis of tunable photonic band structure in an extrinsic plasma photonic crystal," *Phys. E, Low-Dimensional Syst. Nanostruct.*, vol. 67, pp. 7–11, Mar. 2015.
[23] T. Sakaguchi, O. Sakai, and K. Tachibana, "Photonic bands in two-dimensional microplasma arrays. II. Band gaps observed in millimeter and subterahertz ranges," *J. Appl. Phys.*, vol. 101, p. 073305, Apr. 2007.
[24] E. M. Barber, *Aperiodic Structures in Condensed Matter, Fundamentals and Applications*, 1st ed. Boca Raton, FL, USA: CRC Press, 2008.
[25] W. Cai, and V. M. Shalaev, *Optical Metamaterials, Fundamentals and Applications*, 1st ed. New York, NY, USA: Springer-Verlag, 2010.
[26] V. G. Veselago, "The electrodynamics of substances with simultaneously negative values of ε and μ," *Sov. Phys.-Uspekhi*, vol. 10, no. 4, pp. 509–514, Jan. 1968.
[27] J. Li, L. Zhou, C. T. Chan, and P. Sheng, "Photonic Bandgap from a stack of positive and negative index materials," *Phys. Rev. Lett.*, vol. 90, no. 8, p. 083901, Feb. 2003.
[28] H. Jiang, H. Chen, H. Li, Y. Zhang, J. Zi, and S. Zhu, "Properties of one-dimensional photonic crystals containing single-negative materials," *Phys. Rev. E, Stat. Phys. Plasmas Fluids Relat. Interdiscip. Top.*, vol. 69, p. 066607, Jun. 2004.
[29] S. Kocaman *et al.*, "Zero phase delay in negative-refractive-index photonic crystal superlattices," *Nature Photon.*, vol. 5, no. 8, pp. 499–505, Jul. 2011.
[30] F. Xu, and Y. Chen, "Interesting band properties of one-dimensional photonic crystals containing epsilon-negative layers," *Zeitschrift Naturforschung*, vol. 65, no. 4, pp. 329–334, Apr. 2010.
[31] X. Zhang and Y. Chen, "Broadband phase retarder based on one-dimensional photonic crystal containing mu-negative materials," *J. Opt. Soc. Amer. B, Opt. Phys.*, vol. 29, no. 10, pp. 2704–2709, Oct. 2012.
[32] P. Markoš, and C. M. Soukoulis, *Wave Propagation: From Electrons to Photonic Crystals and Left-Handed Materials*, 1st ed. Princeton, NJ, USA: Princeton Univ. Press, 2008.
[33] R. A. Depine, M. L. Martinez-Ricci, J. A. Monsoriu, E. Silvestre, and P. Andres, "Zero permeability and zero permittivity bandgaps in 1D metamaterial photonic crystals," *Phys. Lett. A*, vol. 364, nos. 3–4, pp. 352–355, Apr. 2007.
[34] A. Aghajamali and M. Barati, "Effects of normal and oblique incidence on zero-$\bar{n}$ gap in periodic lossy multilayer containing double-negative materials," *Phys. B*, vol. 407, no. 8, pp. 1287–1291, Apr. 2012.
[35] A. Aghajamali, T. Alamfard, and M. Barati, "Effects of loss factors on zero permeability and zero permittivity gaps in 1D photonic crystal containing DNG materials," *Phys. B*, vol. 454, pp. 170–174, Dec. 2014.
[36] M. Born, and E. Wolf, *Principles of Optics: Electromagnetic Theory of Propagation, Interference and Diffraction of Light*, 7th ed. Cambridge, U.K.: Cambridge Univ. Press, 1999.
[37] C. H. Costa, M. S. Vasconcelos, U. L. Fulco, and E. L. Albuquerque, "Thermal radiation in one-dimensional photonic quasicrystals with graphene," *Opt. Mater.*, vol. 72, pp. 756–764, Oct. 2017.
[38] E. R. Brandão, C. H. Costa, M. S. Vasconcelos, D. H. A. L. Anselmo, and V. D. Mello, "Octonacci photonic quasicrystals," *Opt. Mater.*, vol. 46, pp. 378–383, Aug. 2015.
[39] L. Moretti and F. Scotognella, "Control of the average light transmission in one-dimensional photonic structures by tuning the random layer thickness distribution," *Opt. Mater.*, vol. 46, pp. 450–453, Aug. 2015.
[40] H. G. Booker, *Cold Plasma Waves*, 1st ed. Hingham, MA, USA: Kluwer, 1984.
[41] D. W. Yeh and C. J. Wu, "Thickness-dependent photonic bandgap in a one-dimensional single-negative photonic crystal," *J. Opt. Soc. Amer. B, Opt. Phys.*, vol. 26, no. 8, pp. 1506–1510, Aug. 2009.
[42] H.-Y. Lee and T. Yao, "Design and evaluation of omnidirectional one-dimensional photonic crystals," *J. Appl. Phys.*, vol. 93, no. 2, pp. 819–830, Jan. 2003.
[43] J. S. Pérez-Huerta, D. Ariza-Flores, R. Castro-García, W. L. Mochán, G. P. Ortiz, and V. Agarwal, "Refectivity of 1D photonic crystals: A comparison of computational schemes with experimental results," *Int. J. Mod. Phys. B*, vol. 32, no. 11, p. 1850136, Feb. 2018.
[44] F. Scotognella, "One-dimensional photonic structure with multilayer random defect," *Opt. Mater.*, vol. 36, no. 2, pp. 380–383, Dec. 2013.
[45] Z. N. Dehnavi, H. R. Askari, M. Malekshahi, and D. Dorranian, "Investigation of tunable omnidirectional bandgap in 1D magnetized full plasma photonic crystals," *Phys. Plasmas*, vol. 24, no. 9, p. 093517, Sep. 2017.
[46] S. A. El-Naggar, "Enlarged omnidirectional photonic gap in one dimensional ternary plasma photonic crystals that contains metamaterial," *Eur. Phys. J. D*, vol. 67, no. 3, p. 54, Mar. 2013.

Chittaranjan Nayak received the Ph.D. degree in engineering from the National Institute of Technology, Agartala, India, in 2017.

He is currently an Assistant Professor with the Department of Electronics and Communication Engineering, SRM Institute of Science and Technology, Chennai, India. His current research interests include 1-D photonic multilayers and formation of photonic nanojet for different optoelectronics applications.

Carlos H. Costa received the Ph.D. degree in condensed matter physics from the Department of Physics, Federal University of Rio Grande do Norte, Natal, Brazil, in 2013.

He is currently a Professor with the Federal University of Ceara, Russas, Brazil. His current research interests include magnonic, photonic, and phononic systems, formation and tunneling of band gaps in periodic, quasiperiodic, and random structures.

Alireza Aghajamali received the B.Sc. degree in solid state physics and the master's degree in optics and laser physics from Islamic Azad University, Tehran, Iran, in 2008 and 2011, respectively. He is currently pursuing the Ph.D. degree in physics with Curtin University, Perth, Australia.

His current research interests include atomistic modeling of carbon materials and optical properties of the 1-D photonic crystals.